


Visual processing speed is linked to functional connectivity between right frontoparietal and visual networks

Svenja Küchenhoff¹ | Christian Sorg^{2,3} | Sebastian C. Schneider^{1,2,3} | Oliver Kohl¹ |
Hermann J. Müller¹ | Natan Napiórkowski^{1,4} | Aurore Menegaux^{1,2,3} | Kathrin Finke^{1,4} |
Adriana L. Ruiz-Rizzo¹ 

¹General and Experimental Psychology Unit, Department of Psychology, LMU Munich, Munich, Germany

²Department of Neuroradiology, Technical University of Munich, Munich, Germany

³TUM-Neuroimaging Center, Technical University of Munich, Munich, Germany

⁴Hans-Berger-Clinic of Neurology, Jena University Hospital, Jena, Germany

Correspondence

Adriana L. Ruiz-Rizzo, General and Experimental Psychology Unit, Department of Psychology, LMU Munich, Leopoldstraße 13, 80802 Munich, Germany. Email: adriana.ruiz@lmu.de

Funding information

This work was supported by grants from the German *Forschungsgemeinschaft* to K. F. (grant number FI 1424/2e1) and C. S. (grant number SO 1336/1e1); the European Union's Framework Programme for Research and Innovation Horizon 2020 (2014–2020) under the Marie Skłodowska-Curie Grant Agreements No. 859890 (SmartAge) and No. 754388 (LMUResearchFellows); and from LMUexcellent, funded by the Federal Ministry of Education and Research (BMBF) and the Free State of Bavaria under the Excellence Strategy of the German Federal Government and the Länder.

Abstract

Visual information processing requires an efficient visual attention system. The neural theory of visual attention (TVA) proposes that visual processing speed depends on the coordinated activity between frontoparietal and occipital brain areas. Previous research has shown that the coordinated activity between (i.e., functional connectivity and “inter-FC”) cingulo-opercular (CO_n) and right-frontoparietal (RFP_n) networks is linked to visual processing speed. However, how inter-FC of CO_n and RFP_n with visual networks links to visual processing speed has not been directly addressed yet. Forty-eight healthy adult participants (27 females) underwent resting-state (rs-) fMRI and performed a whole-report psychophysical task. To obtain inter-FC, we analyzed the entire frequency range available in our rs-fMRI data (i.e., 0.01–0.4 Hz) to avoid discarding neural information. Following previous approaches, we analyzed the data across frequency bins (Hz): Slow-5 (0.01–0.027), Slow-4 (0.027–0.073), Slow-3 (0.073–0.198), and Slow-2 (0.198–0.4). We used the mathematical TVA framework to estimate an individual, latent-level visual processing speed parameter. We found that visual processing speed was negatively associated with inter-FC between RFP_n and visual networks in Slow-5 and Slow-2, with no corresponding significant association for inter-FC between CO_n and visual networks. These results provide the first empirical evidence that links inter-FC between RFP_n and visual networks with the visual processing speed parameter. These findings suggest that direct

Abbreviations: ACC, anterior cingulate cortex; BOLD, blood oxygenation level-dependent signal; CO_n, cingulo-opercular network; IC, independent component; ICA, independent component analysis; inter-FC, between-network functional connectivity; NTVA, neural interpretation of TVA; RFP_n, right frontoparietal network; rs-fMRI, resting-state functional magnetic resonance imaging; TVA, theory of visual attention; VPS, visual processing speed.

Kathrin Finke and Adriana L. Ruiz-Rizzo contributed equally to this study.

Edited by: John Foxe

This is an open access article under the terms of the Creative Commons Attribution-NonCommercial License, which permits use, distribution and reproduction in any medium, provided the original work is properly cited and is not used for commercial purposes.

© 2021 The Authors. *European Journal of Neuroscience* published by Federation of European Neuroscience Societies and John Wiley & Sons Ltd.

connectivity between occipital and right frontoparietal, but not fronto-insular, regions support visual processing speed.

KEYWORDS

between-network connectivity, cingulo-opercular network, resting-state fMRI, theory of visual attention, visual attention

1 | INTRODUCTION

Visual information processing requires an efficient visual attention system. The speed of information uptake in a given unit of time, an index of attentional capacity, can be estimated using the mathematical framework of the “theory of visual attention” (TVA; Bundesen, 1990). Within the TVA framework, visual processing speed (VPS) is estimated based on an individual's accuracy in a whole-report task requiring the observer, without emphasis on speed, to report as many letters as possible from briefly presented displays that vary in duration. The estimated VPS represents a latent-level parameter that is relatively constant across diverse conditions (e.g., Finke et al., 2005). In the neural interpretation of TVA (NTVA; Bundesen et al., 2005), it is assumed that the computations that determine VPS, that is, the selection of relevant visual features, are generated in frontal, parietal, and/or limbic (control) areas and projected to occipital (visual-coding) areas. A prior independent, exploratory resting-state functional magnetic resonance imaging (MRI) (rs-fMRI) study showed, *post-hoc*, that VPS relates to the inter-network functional connectivity (inter-FC) between the cingulo-opercular (CON) and the right frontoparietal (RFPn) networks (Ruiz-Rizzo et al., 2018)—both of which comprise frontal, parietal, and limbic areas. However, the link between VPS and the inter-FC of CON and RFPn, respectively, with *occipital* areas has not yet been directly and systematically addressed. The demonstration of such a link would provide the missing key empirical evidence for the NTVA's theoretical assumption of the projection of the feature selection parameter settings from higher-order to occipital areas. Thus, the present study set out to test whether such a link indeed exists.

Previous studies have shown that CON and RFPn interact with occipital areas. For example, CON regions, such as the prefrontal, insular, and midcingulate cortices (Dosenbach et al., 2008; Seeley et al., 2007), increase their functional connectivity with the occipital cortex during eyes open vs. eyes closed (Riedl et al., 2016). These regions exhibit sustained activity in tasks involving active visual processing (Sestieri et al., 2013). Similarly, the volume of the white matter tracts underlying RFPn regions (i.e., dorsolateral prefrontal cortex and areas around the intraparietal sulcus; Dosenbach et al., 2007) predict faster stimulus detection in visuospatial

attention tasks (Thiebaut de Schotten et al., 2011), and more right-hemispheric lateralization of the inferior fronto-occipital fasciculus has been associated with higher values of the TVA-based VPS parameter (Chechlacz et al., 2015). Building on this prior evidence, the previously shown relevance of, specifically, CON and RFPn for VPS (Ruiz-Rizzo et al., 2018), and the theoretical proposal of the neural TVA on how VPS is implemented at the neural level (NTVA; Bundesen et al., 2005), the present study addressed the question of how inter-FC of, specifically, CON and RFPn with occipital regions support VPS.

Rs-fMRI allows measuring the correlation between brain regions' spontaneous (i.e., intrinsic) hemodynamic activity, which reflects fluctuations in cortical excitability (Raichle, 2011). We, thus, used rs-fMRI to study the intrinsic inter-FC of CON and RFPn with visual networks. Rs-fMRI data are typically temporally filtered (0.01–0.1 Hz) to remove non-neural scanner signal drifts (low frequencies) and cardio-respiratory signals (high frequencies) (Cordes et al., 2001). However, the spectral centroid (or “center of gravity” of the frequencies) of CON, RFPn, and visual networks lies around the *upper* limit of the traditionally filtered frequency range (i.e., 0.098, 0.090, and 0.090–0.118 Hz, respectively; Ries et al., 2018). Further, *within*-network functional connectivity can be stronger in the typical range (<0.08 Hz) for dorsal prefrontal regions (RFPn), but above 0.08 Hz for insular and orbitofrontal areas (CON, Salvador et al., 2008).

Previous rs-fMRI studies (e.g., Gohel & Biswal, 2015; Wang et al., 2018; Zuo et al., 2010) have examined all frequencies in their signal by adopting the slowest, supra-second oscillatory ranges derived from electrophysiological measures of neuronal activity (Penttonen & Buzsáki, 2003). This approach has revealed a similar spatial extent of functional connectivity *within* CON, RFPn, and visual networks across frequencies, with most of their total power in intermediate ranges (i.e., 0.073–0.198 Hz; Gohel & Biswal, 2015). Following this approach, here we used the entire frequency spectrum available in our rs-fMRI data (i.e., 0.01–0.4 Hz) and analyzed inter-FC across discrete frequency bins, including one “reference” bin (i.e., entire spectrum). We expected significant inter-FC between CON, RFPn, and visual networks across frequency bins (Gohel & Biswal, 2015; Wang et al., 2018). We furthermore expected the inter-FC of CON

and RFPn (respectively) with visual networks to be significantly linked to VPS. Finally, we explored whether this link is frequency specific.

2 | MATERIALS AND METHODS

2.1 | Participants

Forty-eight healthy adults (age range: 20–50 years; 27 females), taken from the “INDIREA” Munich cohort published in Ruiz-Rizzo et al., (2019), were included in the current study (see demographic information in Table 1), although the current hypotheses and analyses were generated independently. The study was approved by the ethics committee of the Faculty of Psychology and Educational Sciences of LMU Munich, and all participants provided written informed consent. To avoid strong age effects (e.g., on the VPS parameter; McAvinue et al., 2012), we selected all participants younger than 50 years from the original cohort. All of them exhibited normal psychomotor speed performance in a neuropsychological paper-and-pencil task (TMT-A, Reitan, 1958; Tombaugh, 2004); all had normal or corrected-to-normal visual acuity, and none was suffering from psychological or neurological disorders potentially affecting cognition, or from diabetes or color blindness. To further ensure health status, participants additionally completed demographic and behavioral (e.g., Beck Depression Inventory [BDI]; Deutsche Bearbeitung von Beck et al., 1996; Hautzinger et al., 2009) self-report questionnaires, as well as a test of crystallized intelligence (i.e., the multiple-choice vocabulary test: “Mehrfachwahl-Wortschatz-Test”; Lehrl et al., 1999). Thus, we assumed the relationship between inter-FC and our TVA-based measure of VPS to be uncontaminated by potential pathological influences.

TABLE 1 Demographic variables

Variable (<i>N</i> = 48)	Mean ± <i>SD</i>
Age (years)	32.96 ± 9.58
Sex (female/male)	27/21
Education (years)	12.21 ± 1.07
Intelligence (IQ)	110.30 ± 14.05
Depression (BDI score)	4.96 ± 4.80
Handedness	0.71 ± 0.55
TMT-A (time in s)	25.53 ± 10.71

Notes: Handedness: 1, completely right handed; –1, completely left-handed; BDI cutoff: 19. TMT-A mean and *SD* correspond with those reported in (Tombaugh, 2004).

Abbreviations: BDI, Beck Depression Inventory (Deutsche Bearbeitung von Beck et al., 1996; Hautzinger et al., 2009); *SD*, standard deviation; TMT-A, Trail-Making Test Part A.

Details on data acquisition are reported elsewhere (Ruiz-Rizzo et al., 2019). Briefly, after screening for inclusion and exclusion criteria, participants underwent rs-fMRI at the *Klinikum rechts der Isar* (Munich, Germany) in a first session. In a second session, participants performed the TVA-based whole-report task.

2.2 | Experimental design and statistical analyses

2.2.1 | Assessment and estimation of VPS parameter *C*

A whole-report task based on TVA (Bundesen, 1990) was used to estimate the TVA VPS parameter or parameter “*C*”. In this task, arrays of four letters were presented in an imaginary semicircle under different exposure durations determined in a pretest before the actual task. To identify individual shortest exposure durations, we used a staircase procedure in the pretest, which included four blocks of 12 trials each: four “adjustment” trials, four trials with unmasked displays presented for 200 ms, and four masked displays presented for 250 ms. Each block started with one (of four) adjustment trial displayed for 80 ms, immediately followed by a post-display mask (see below). If the participant reported at least one letter correctly, the exposure duration was decreased by 10 ms in the following three adjustment trials within each block, until the participant could no longer report one letter correctly (i.e., the shortest exposure duration). If this point was reached before the last of the 16 adjustment trials, the exposure duration was held constant for the remaining. Setting the exposure duration that short ensured obtaining a valid estimate of the visual perceptual threshold parameter. Then, based on the shortest exposure duration, longer values were added to obtain report performance across the whole range from near-floor to near-ceiling and thus allow for a more precise TVA-based parameter estimation. In the actual whole-report task, on each trial, red letters were presented on either the left or the right side (counterbalanced) of a fixation point located in the screen center (Figure 1). Four blue non-letter items (i.e., abstract shapes made of letter parts) were presented on the corresponding opposite site to balance visual stimulation.¹ Letter stimuli were randomly chosen from the set

¹This was necessary, as the task was performed during electroencephalographic (EEG) recordings where lateralized event-related EEG components were assessed. Note that this procedure did not compromise the whole-report nature of the task (i.e., cannot be taken to resemble a partial-report task) because the letter stimuli were presented on one side of the screen (and the abstract items on the other side) for the duration of an experimental block, and the instruction was to report all letters—with opposite-site abstract items not fulfilling this criterion and being of a different color.

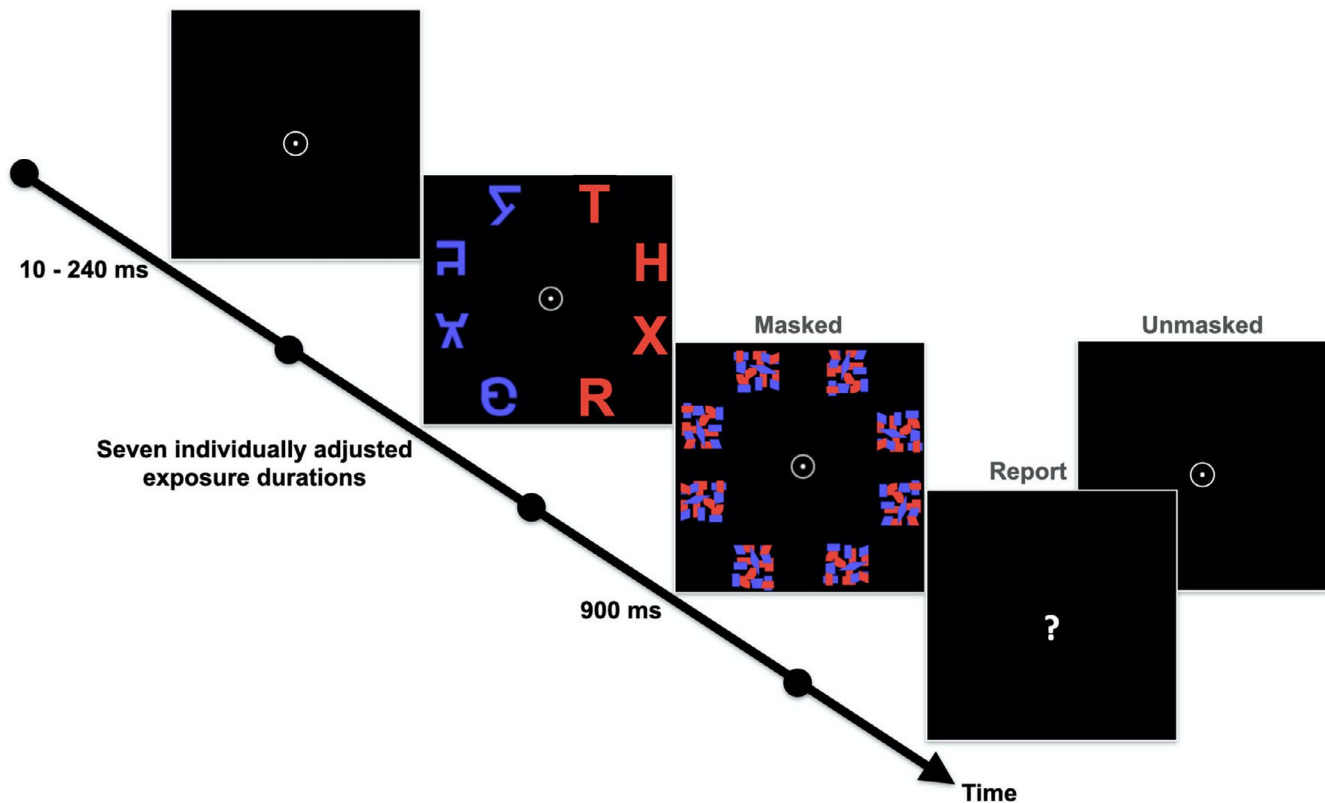


FIGURE 1 Whole-report task used to estimate the visual processing speed parameter C . In this task, semicircular arrays of letters are presented under seven exposure durations determined in a pretest for each participant. Participants are asked to report all letters they are fairly certain they have seen, placing emphasis on accuracy, and not speed, of verbal report. In 15 of the 40 trials within a block, masks immediately followed stimuli presentation. The remaining 25 block trials were unmasked to add a component of iconic memory buffering to the TVA estimation. Non-letter items were presented on the corresponding opposite site to balance visual stimulation

(A, B, D, E, F, G, H, J, K, L, M, N, O, P, R, S, T, V, X). In a given trial, a particular letter appeared only once, and each letter was equally frequent within a block. Participants were instructed to report, verbally, all letters they were “fairly certain” they had seen (i.e., to avoid too conservative or too liberal a report criterion). Only report accuracy, but not report order or speed, was considered to assess performance.

The task consisted of 400 trials, split into ten blocks of 40 trials each. Within a block, in fifteen of the trials, masks immediately followed stimuli presentation. These masks were jumbled blue and red squares, presented for 900 ms at each stimulus location to counteract visual persistence (Figure 1). Masked trials were presented for five different exposure durations (three times each). The use of varying exposure durations set for each individual was intended to increase precision in the TVA-based parameter estimation by allowing variability in report performance. The remaining 25 block trials were unmasked to add a component of iconic memory buffering (Sperling, 1960) to the estimation and ensure a valid and reliable TVA parameter fitting. These unmasked trials were presented for either the second shortest masked duration (three trials) or 200 ms (22 trials)—we chose the

duration of 200 ms because electroencephalographic measures were simultaneously obtained to analyze event-related potentials (not reported in this study). Furthermore, as the shortest trial was too brief for visual perception, the second shortest was presented. Hence, in each block, trials were presented for seven *effective* exposure durations (five masked and two unmasked).

The VPS parameter, C , was estimated by modeling participants' report accuracy as a function of the effective exposure duration, using a maximum likelihood-fitting algorithm (Bundesen, 1990; Dyrholm et al., 2011; Kyllingsbæk, 2006). Specifically, performance was modeled by an exponential growth function characterizing the increase in the probability of correct letter report with increasing effective exposure duration. The VPS parameter C represents the rate of uptake of visual information (in numbers of elements per second) and is given by the function's slope at its origin. Although not in the focus of the present study, three additional parameters were estimated, namely, parameter t_0 , parameter K , and parameter μ . Parameter t_0 , the function's origin, indicates the longest exposure duration (in ms) below which information uptake is effectively zero and represents the visual perceptual

threshold. Parameter K , the function's asymptote, indicates the maximum number of elements that can be simultaneously encoded in the visual short-term memory store. Parameter μ reflects the duration of iconic memory buffering in unmasked trials.

2.2.2 | Statistical analyses

To statistically compare networks' inter-FC Z values across frequency bins, we performed repeated-measures analyses of variance (ANOVA), one for each relevant network pair, with frequency bins as the within-subject factor and Z values for a particular network pair as the dependent variable. The relevant network pairs were CON and visual networks, RFPn and visual networks, CON and RFPn, and all visual networks. After each repeated-measures ANOVA, *post-hoc* tests were performed on individual Z values for the respective network pairs. When Mauchly's test indicated that the assumption of sphericity had been violated, Greenhouse-Geisser correction was applied. Bonferroni correction ($p_{0.05/6} = 0.008$ for comparisons involving CON, $p_{0.05/3} = 0.017$ for the rest of networks) was applied to *post-hoc* paired-sample t tests. These analyses were performed in R 4.0.0 (R Core Team, 2020; <https://www.R-project.org/>; R. Studio v. 1.2.5042; RStudio Team, 2020; <https://www.rstudio.com/>).

We analyzed the relationship between inter-FC of CON and RFPn with visual networks and VPS parameter C by multiple regressions. Specifically, individual values of C were predicted from inter-FC Z values in each frequency bin (Slow-5, Slow-4, Slow-3, Slow-2), frequencies altogether (henceforth named "Global"; see 2.5 Temporal filtering of rs-fMRI data below), age (as after exclusion of high age the range was still 30 years), and framewise displacement (a measure of head movement in the scanner from frame to frame). Five multiple regression models were tested, one for each visual network's inter-FC with CON and RFPn. Therefore, each model consisted of 13 predictors: six for the inter-FC of CON with a particular visual network across frequency bins and global; five for the inter-FC of RFPn with the same visual network across frequency bins and global; one for age; and one for framewise displacement. Note that the predictors involving CON were six instead of five because there were two subcomponents of CON in Slow-3 instead of one (see 3.1 Brain network selection in the Results section). The goal of this analysis was to determine whether any of the predictors (i.e., inter-FC between a visual network and CON and RFPn, across frequency bins) in any of the models (i.e., that differed by visual network) was associated with parameter C —as we had no priors about one specific visual network or frequency bin being more relevant than the others. Including all frequency bins in one regression model allowed us to determine whether those associations were frequency specific and/or specific to CON

or RFPn, as (unlike in separate bivariate correlations) the effect of each predictor is accounted for in the model. Next, we compared the beta coefficients in the models where significant predictors were found with linear *post-hoc* contrasts. Results were deemed significant if $p < 0.05$.

2.3 | MRI data acquisition

Image acquisition was conducted on a Philips Ingenia 3 T MRI scanner (Philips Healthcare, Best, the Netherlands) with a standard 32-channel SENSE head coil, located in the *Klinikum rechts der Isar*, Munich (Germany). During the rs-fMRI session, participants were asked to try to avoid thinking about anything in particular, moving, or falling asleep. Head motion was restrained throughout the scanning session by foam padding around participants' heads, and scanner noise was reduced by providing participants with earplugs and headphones. Six-hundred T2*-weighted blood oxygenation level-dependent (BOLD)-fMRI volumes were acquired per participant, using a multiband echo-planar imaging (EPI) sequence, with a 2-fold in-plane SENSE acceleration (SENSE factor, $S = 2$; Preibisch et al., 2015) and an M-factor of 2 (repetition time, 1,250 ms; time to echo, 30 ms; flip angle, 70°; 40 slices; 3-mm slice thickness and 0.3-mm inter-slice gap; voxel size, $3 \times 3 \times 3.29 \text{ mm}^3$; matrix size, 64×64). Anatomical detail was achieved by a higher resolution T1-weighted volume, acquired with a 3D magnetization prepared rapid acquisition gradient echo (MPRAGE) sequence (repetition time, 9 ms; time to echo, 4 ms; flip angle, 8°; 170 slices; voxel size, 1 mm^3 ; matrix size, 240×240).

2.4 | Rs-fMRI data preprocessing

As we were interested in examining frequencies that could also include physiological non-neural (e.g., respiratory) or scanner "noise" signals (e.g., $>0.1 \text{ Hz}$), we reduced the possibility of including those non-neural signals by applying physiologic estimation by temporal independent component (IC) analysis (PESTICA; Beall & Lowe, 2007; <https://www.nitrc.org/projects/pestica>). PESTICA estimates the breathing and pulse signals from the data by performing slice-wise temporal ICA, identifying noise components per slice, and implementing signal correction (Beall & Lowe, 2007). We used this approach because no respiratory or cardiac signals were directly measured during rs-fMRI and before the standard preprocessing, as recommended.

Next, we pre-processed the PESTICA-corrected rs-fMRI data using Data Processing Assistant for Resting-State fMRI (DPARSF) (Yan & Zang, 2010; <https://www.nitrc.org/projects/dparsf/>), which is based on SPM12 software (Statistical Parametric Mapping; Penny et al., 2011;

ion.ucl.ac.uk/spm/software/spm12/), running on MATLAB (2016a, The Mathworks, Inc., Natick, USA). The preprocessing steps included discarding the first five volumes to remove initial T1 saturation; slice-timing correction; reorienting to anterior commissure–posterior commissure plane; realignment; co-registration to the high-resolution, structural image; DARTEL (Diffeomorphic Anatomical Registration using exponentiated Lie algebra; Ashburner, 2007) segmentation into the three tissue types (gray matter, white matter, and cerebrospinal fluid); normalization to the Montreal Neurological Institute (MNI) space; spatial smoothing with a 4-mm full-width-at-half-maximum Gaussian kernel and detrending. Moreover, the signals from white matter and cerebrospinal fluid, the six head motion parameters and their corresponding first derivatives, and the “bad” frames (based on the framewise displacement metric of Power et al., 2012, as implemented in DPARSF) were regressed out from the rs-fMRI data. The global signal was not regressed out during preprocessing to avoid possible spurious anticorrelations.

2.5 | Temporal filtering of rs-fMRI data

Following the frequency ranges of the slowest oscillations as defined in Penttonen and Buzsáki (2003) and on previous rs-fMRI studies (e.g., Gohel & Biswal, 2015; Zuo et al., 2010), we focused on four frequency bins: “Slow-5” (0.01–0.027 Hz), “Slow-4” (0.027–0.073 Hz), “Slow-3” (0.073–0.198 Hz), and “Slow-2” (0.198–0.4 Hz). The upper limit of Slow-2, and our highest frequency possible, was defined based on the Nyquist frequency for our 1.25-s repetition time, that is, $(1/1.25)/2$ Hz. The current sampling frequency did not permit including the actual upper limit of Slow-2 (i.e., 0.5 Hz), and “Slow-1” (0.5–0.75 Hz) (cf. Gohel & Biswal, 2015). We used these bins to temporally filter the preprocessed data. Thus, we obtained five data versions, each with a different frequency composition, namely, the four frequency bins and one “Global,” encompassing all bins (i.e., 0.01–0.4 Hz) and, hence, being virtually equivalent to unfiltered data, for comparison (similar to the approach by Gohel & Biswal, 2015). Note that these versions solely differed in their spectral content and that global was included as a reference, to better appreciate the possible frequency specificity of inter-FC, and its association with VPS.

2.6 | IC analysis and dual regression

Spatial group ICA was used to decompose the preprocessed BOLD-fMRI volumes into 75 spatially ICs and their related non-orthogonal time courses (McKeown et al., 1998) with FSL (v. 5.0.7; Jenkinson et al., 2012) MELODIC (v. 3.14; Smith et al., 2004). The number of ICs was chosen following

Allen et al., (2011), who identified all resting-state networks relevant for our study. Dual regression was performed on all ICs to generate participant-specific time courses (Stage 1) and spatial maps (Stage 2) (Beckmann et al., 2009). The participant-specific time courses were used as input for the inter-FC analysis. Both ICA and dual regression were performed separately for each of the four frequency bins and for the global data.

2.7 | Brain network selection

For each frequency bin, we obtained the ICs' spatial cross-correlation values with resting-state network templates (Allen et al., 2011) using FSL's *fsfcc* command (https://surfer.nmr.mgh.harvard.edu/pub/dist/freesurfer/tutorial_packages/OSX/fsl_501/src/avwutils/fslcc.cc). As we were interested only in networks previously shown relevant for VPS (Haupt et al., 2020; Ruiz-Rizzo et al., 2018), we selected the two ICs, as defined in Allen et al., (2011), that showed the highest correlation coefficients with, correspondingly, CON (Allen et al.'s Saliency, IC 55), RFPn (Allen et al.'s IC 60), and visual networks (Allen et al.'s IC 39, IC 46, IC 48, IC 59, IC 64, and IC 67). Note that we did not exhaustively select *all* brain networks relevant for attention (e.g., the dorsal attention network or the bilateral executive control network) but only those that have been specifically associated with VPS. Next, the two ICs that correlated the highest were visually inspected and the one including the most relevant regions of each network were chosen. These regions included the anterior insula and anterior midcingulate cortex for CON; the right middle frontal gyrus and anterior inferior parietal lobule for RFPn; and striate and extrastriate cortex, as well as lateral geniculate nucleus of the thalamus, for the visual networks (Uddin et al., 2019). After visual inspection, if both ICs included parts of the relevant regions in a complementary manner (i.e., the network was split), both were selected. If both ICs included the relevant regions, but these were unidentifiable from the overall spatial pattern of the IC (i.e., the ICs additionally included other brain regions or noise patterns), none was selected.

2.8 | Inter-FC analyses

To calculate the individual inter-FC of network pairs, the specific time courses (i.e., those derived from Stage 1 of the dual regression) of the networks of interest were correlated for each participant. The resulting *r* value matrices were Fisher *Z* transformed and averaged across participants to obtain a group-level inter-FC matrix. One-sample *t* tests were computed on the group mean Fisher-*Z*-transformed correlation matrix and the false discovery rate (FDR) method

(Benjamini & Hochberg, 1995) was used to correct for multiple comparisons ($p < 0.05$ and $q < 0.05$). We repeated this step for each frequency bin (including global). This analysis was performed with custom code written in MATLAB (Ruiz-Rizzo & Küchenhoff, 2020).

2.9 | Code accessibility

Analysis scripts for the inter-FC and the statistical analyses and analyzed neuroimaging data are publicly available and can be accessed online (<https://osf.io/nhqq3/>). Analyzed behavioral data will also be accessible to qualified researchers upon request.

3 | RESULTS

3.1 | Brain network selection

Coefficients for the cross-correlation of ICs with the network templates of Allen et al., (2011) are listed in Table 2. CON was consistently identified across all frequency bins and global. For Slow-3, two subcomponents of CON were identified, one centered on the insula and the other on the anterior cingulate cortex (ACC) (Figure 2a, top row, third column; IC32 and IC42, respectively). Thus, both ICs (i.e., IC32 and IC42) were included in further analyses. RFPn was consistently identified across all frequency bins and Global

(Figure 2a, bottom row). Finally, five (out of six) of Allen et al.'s visual system networks (named here as Vis-39, Vis-46, Vis-59, Vis-64, and Vis-67 following Allen et al.'s IC numbering) were consistently identified across all frequency bins and global (Figure 2b). Allen et al.'s IC 48 could be identified only in global and Slow-4 and, thus, was excluded from further analyses.

3.2 | Inter-FC between CON, RFPn, and visual networks

The group average correlation matrix, per frequency bin, between CON, RFPn, and visual networks is depicted in Figure 3, and the corresponding statistical comparison across frequency bins, for CON, RFPn, and visual network pairs is shown in Figure 4. CON exhibited significant inter-FC with three visual networks (Vis-39, Vis-59, and Vis-67) in three frequency bins: Slow-4, Slow-3, and Slow-2. The inter-FC with Vis-39 was negative in both Slow-4 ($Z = -0.28$, $p < 0.001$) and Slow-2 ($Z = -0.09$, $p = 0.004$). The inter-FC with Vis-59 was negative in Slow-4 ($Z = -0.16$, $p < 0.001$) and positive in Slow-3 (ACC-subcomponent: $Z = 0.08$, $p = 0.011$; insula-subcomponent: $Z = 0.14$, $p < 0.001$). Finally, the inter-FC with Vis-67 was also negative in Slow-4 ($Z = -0.12$, $p = 0.004$) and positive in Slow-3 (insula-subcomponent: $Z = 0.12$, $p < 0.001$). As a reference, when all frequencies were considered together (i.e., global), CON exhibited significant negative inter-FC with Vis-39 ($Z = -0.12$,

TABLE 2 ICs with highest correlation coefficients with network templates across frequency bins (and global, for comparison)

Network template	Frequency bin				
	Slow-5	Slow-4	Slow-3	Slow-2	Global
CON	IC20 (0.63)	IC32 (0.52)	IC32 (0.38)	IC51 (0.27)	IC27 (0.39)
	IC15 (0.24)	IC35 (0.41)	IC42 (0.31)	IC23 (0.24)	IC44 (0.36)
RFPn	IC7 (0.64)	IC4 (0.70)	IC2 (0.72)	IC61 (0.43)	IC3 (0.69)
	IC14 (0.25)	IC18 (0.21)	IC33 (0.27)	IC58 (0.26)	IC15 (0.33)
Vis-39	IC11 (0.49)	IC20 (0.43)	IC3 (0.44)	IC52 (0.28)	IC4 (0.49)
	IC14 (0.28)	IC40 (0.43)	IC33 (0.35)	IC40 (0.22)	IC15 (0.28)
Vis-46	IC2 (0.49)	IC8 (0.58)	IC5 (0.47)	IC11 (0.47)	IC5 (0.46)
	IC1 (0.35)	IC2 (0.36)	IC10 (0.39)	IC10 (0.31)	IC11 (0.44)
Vis-59	IC1 (0.51)	IC6 (0.47)	IC4 (0.54)	IC2 (0.51)	IC1 (0.52)
	IC32 (0.32)	IC17 (0.39)	IC63 (0.29)	IC3 (0.25)	IC28 (0.33)
Vis-64	IC5 (0.55)	IC1 (0.64)	IC5 (0.51)	IC8 (0.49)	IC5 (0.48)
	IC2 (0.44)	IC6 (0.35)	IC4 (0.41)	IC10 (0.37)	IC14 (0.45)
Vis-67	IC18 (0.47)	IC2 (0.48)	IC40 (0.48)	IC44 (0.44)	IC38 (0.44)
	IC43 (0.33)	IC39 (0.36)	IC10 (0.30)	IC8 (0.31)	IC14 (0.38)

Note: Correlation coefficients between Allen et al., (2011)'s templates and the two independent components (ICs) with the highest values are shown separately for networks of interest and frequency bins. Selected ICs (based on correlation coefficients and visual inspection) are marked in bold. Allen et al.'s Saliency (IC 55) and Right frontoparietal network (IC 60) correspond to the cingulo-opercular network (CON) and right frontoparietal network (RFPn), respectively, of the present study. Slow-5:0.01–0.027 Hz; Slow-4:0.027–0.073 Hz; Slow-3:0.073–0.198 Hz; Slow-2:0.198–0.4 Hz. Vis, visual networks.

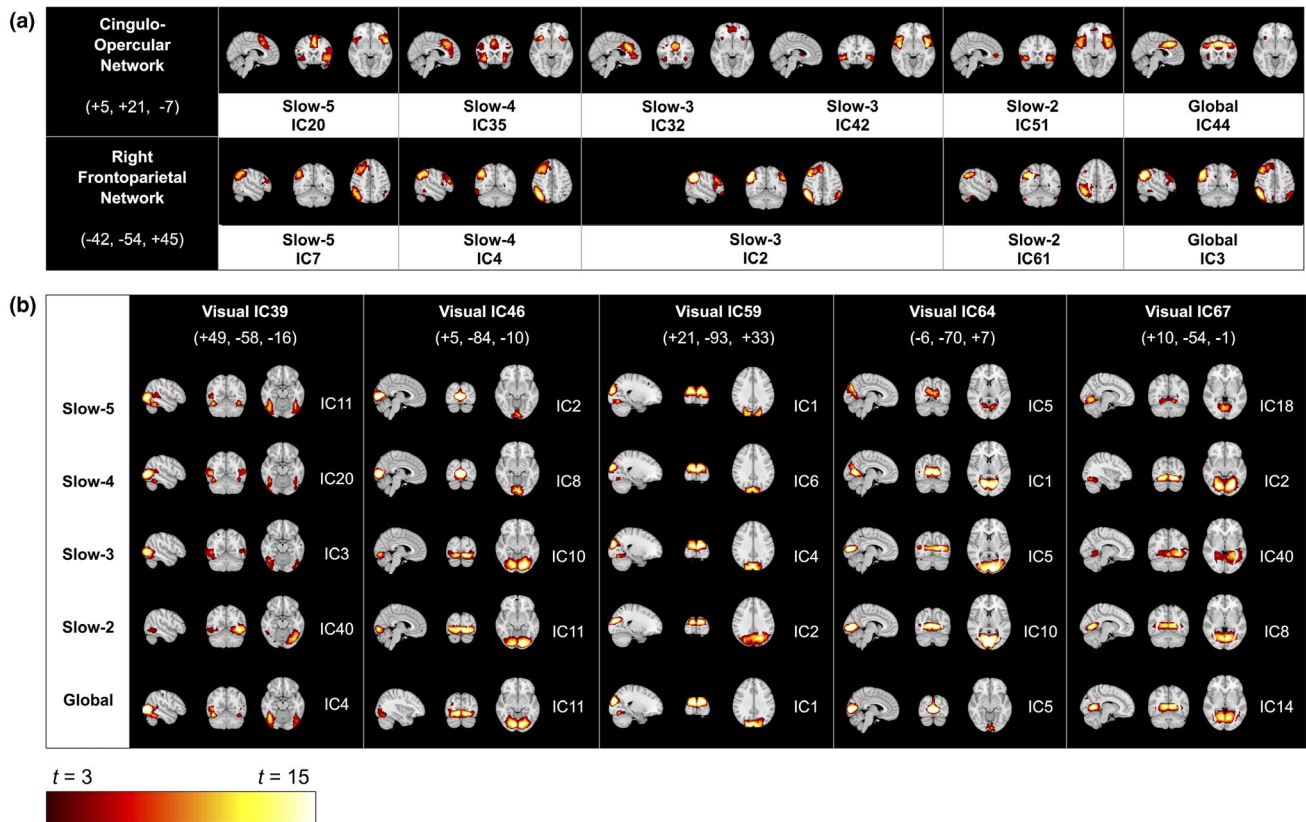


FIGURE 2 Networks of interest identified for each frequency bin. Independent components (ICs) representative of the cingulo-opercular and right frontoparietal networks (a) and visual networks (b) (following Allen et al., 2011) in each frequency bin (Slow-5 to Slow-2) and global, for comparison. Montreal Neurological Institute coordinates (x, y, z , in mm) correspond to the slices shown for each network. Slow-5:0.01–0.027 Hz; Slow-4:0.027–0.073 Hz; Slow-3:0.073–0.198 Hz; Slow-2:0.198–0.4 Hz. Brain images are shown in radiological orientation (right hemisphere on the left)

$p < 0.0001$) and Vis-59 ($Z = -0.10, p < 0.0001$) and positive with Vis-46 ($Z = 0.07, p = 0.004$). When comparing across frequency bins (Figure 4a), we found the average inter-FC between CON and visual networks to differ significantly ($F[3.38, 812.6] = 33.67, p < 0.001, \eta^2 = 0.09$). In particular, the (positive) inter-FC between CON's insula-subcomponent and visual networks in Slow-3 was significantly stronger compared with the inter-FC between (single component) CON and visual networks in all other frequency bins (all Bonferroni-corrected p values < 0.001), though it was comparable in magnitude (i.e., absolute value) to the negative inter-FC between CON and visual networks in Slow-4 ($t(47) = -1.19, p = 0.241$).

RFPn exhibited significant negative inter-FC with the same three visual networks as CON (Vis-39, Vis-59, and Vis-67) in all frequency bins (Figure 3; e.g., Vis-59: $Z = -0.38$ in Slow-5; Vis-39: $Z = -0.35$ in Slow-4; Vis-67: $Z = -0.10$ in Slow-3; all p values < 0.001) but Slow-2, in which the only significant inter-FC was observed with Vis-46 ($Z = -0.07, p = 0.021$). As a reference, in global, RFPn showed significant negative inter-FC with all visual networks (Z values' range: -0.37 to -0.19 ; all p values < 0.0001). When comparing across frequency bins (Figure 4b), we again found the

inter-FC between RFPn and visual networks to differ significantly ($F[2.28, 544.92] = 50.94, p < 0.001, \eta^2 = 0.11$). In particular, the mean inter-FC was decreasingly less negative with increasing frequency, indicating that correlations were stronger and more negative in slower than in faster frequency bins. Bonferroni-corrected *post-hoc* tests revealed that inter-FC between RFPn and visual networks was equally strong in Slow-5 (mean $Z = -0.25$) and Slow-4 (mean $Z = -0.23$), but decreased in magnitude in Slow-3 (mean $Z = -0.12, p < 0.0001$, in comparison with all other bins) and Slow-2 (mean $Z = -0.02, p < 0.001$, in comparison with all other bins).

CON showed significant inter-FC with RFPn in the following frequency bins (Figure 3): positive in Slow-4 ($Z = 0.19, p < 0.0001$) and Slow-3 (ACC-subcomponent: $Z = 0.15, p < 0.0001$), and negative in Slow-2 ($Z = -0.13, p < 0.001$). In Slow-5, inter-FC with RFPn was non-significant ($Z = -0.08, p = 0.065$). As a reference, in global, the inter-FC between these two networks was positive ($Z = 0.08, p < 0.001$). Comparison across frequency bins (Figure 4c) revealed the inter-FC between RFPn and CON to differ significantly ($F[2.90, 136.49] = 18.30, p < 0.001, \eta^2 = 0.24$). Bonferroni-corrected *post-hoc* tests showed that the inter-FC

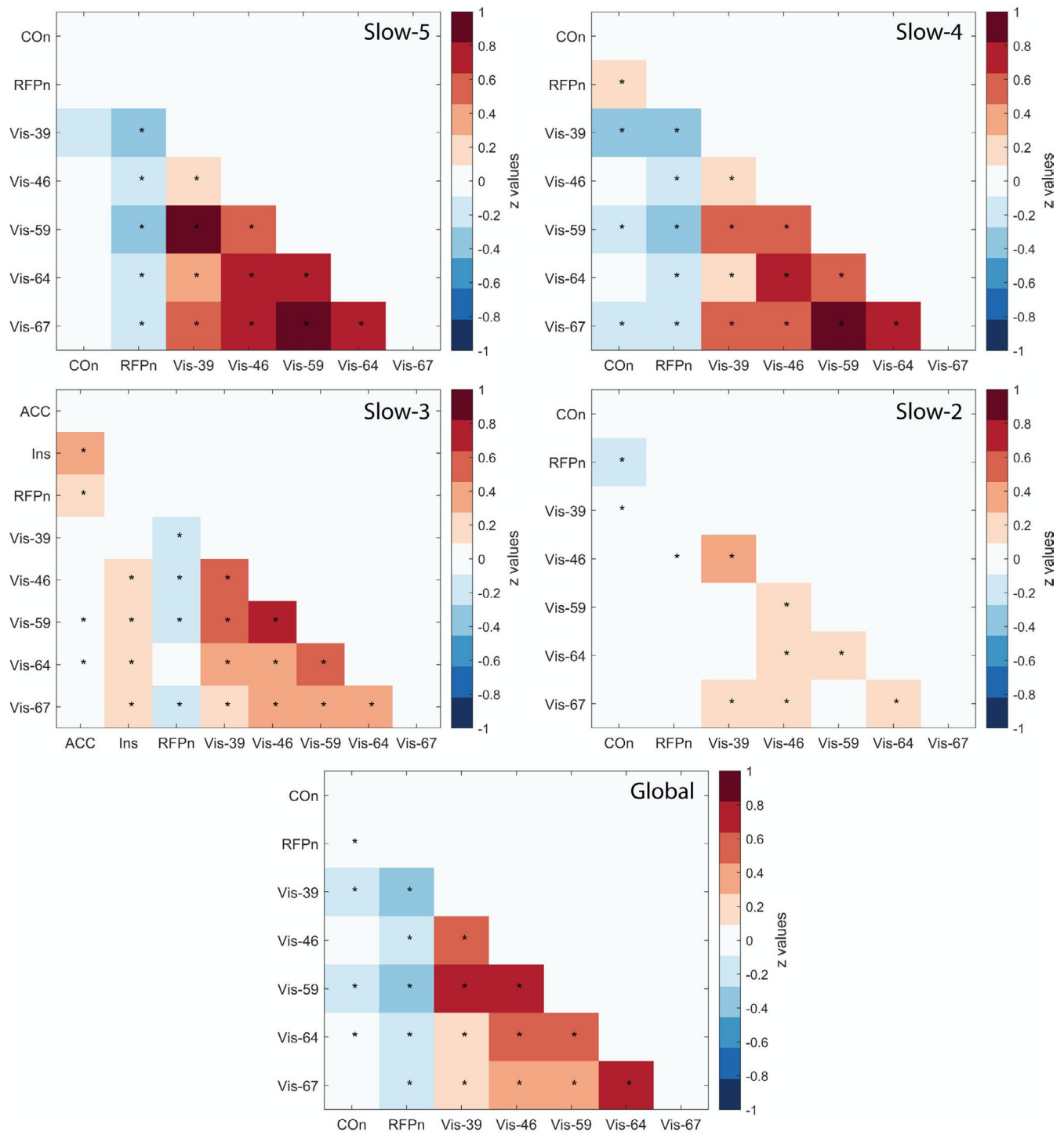


FIGURE 3 Group average correlation matrices between visual processing speed (VPS) relevant networks. Correlation matrices representing functional connectivity (Z values) between higher order networks previously shown relevant for VPS (cingulo-opercular network, COOn, and right frontoparietal network, RFPn) and visual networks (Vis) across frequency bins (Slow-5 to Slow-2) and global (frequencies altogether), for reference. Red indicates positive correlations, whereas blue and white indicate, respectively, negative and around-zero correlations. False discovery rate (FDR)-corrected ($q < 0.05$) significant values are marked with a “*”. See text for specific frequency ranges included in each bin

between RFPn and COOn was significantly more positive in Slow-4 and Slow-3 (ACC-subcomponent only) than in the other frequency bins or the insula-subcomponent in Slow-3 (all p values < 0.001 ; Figure 4c).

Finally, for all visual networks, there was positive inter-FC throughout the entire frequency range (range: $Z = 0.84$ in Slow-5 to 0.06 in Slow-2; Figure 3). As a reference, in global, the inter-FC among all visual networks

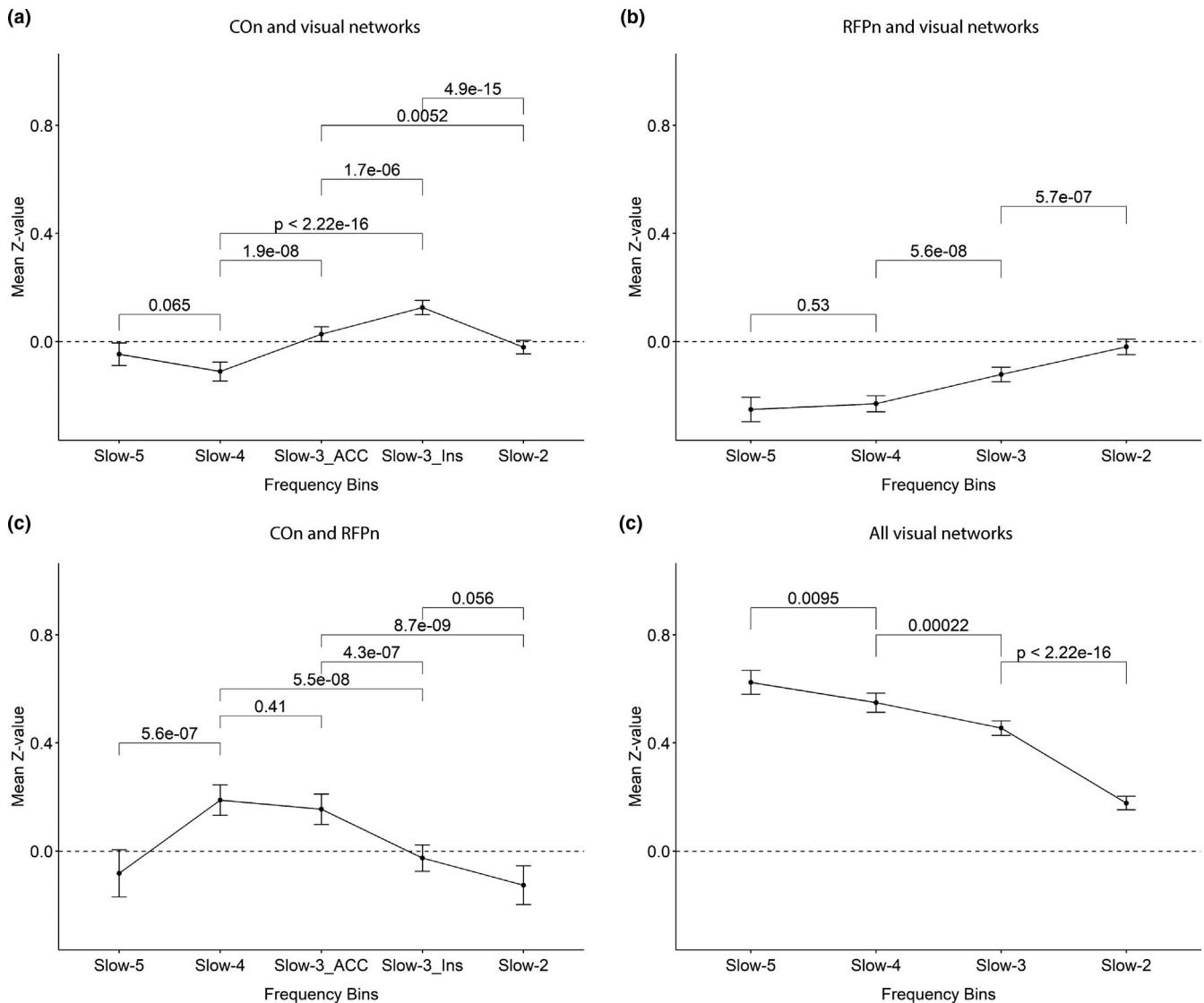


FIGURE 4 Mean inter-functional connectivity (FC) between cingulo-opercular, right frontoparietal, and visual networks across frequency bins. (a) The mean Z value of the inter-FC between the cingulo-opercular (CO_n) and all visual networks was strongest in Slow-3 (positive) with the CO_n's insula-subcomponent (Slow-3_Ins) and Slow-4 (negative). (b) The mean Z value of the inter-FC between the right frontoparietal network (RFP_n) and all visual networks was negative and strongest in Slow-5 and Slow-4. (c) The mean Z value of the inter-FC between CO_n and RFP_n was positive and strongest in Slow-4 and Slow-3 with the CO_n's anterior cingulate cortex (ACC)-subcomponent (Slow-3_ACC). (d) The mean Z value of the inter-FC among visual networks was positive and strongest in Slow-5. Significance was determined at Bonferroni-corrected $p_{0.05/6} = 0.008$ (for a and c, where CO_n was subdivided into two subcomponents) and $p_{0.05/3} = 0.017$ (for b and d). Bars represent 95% confidence intervals

was significantly positive, too (Z values' range: 0.75 [Vis-59 and Vis-46] to 0.12 [Vis-39 and Vis-67]). When comparing across frequency bins (Figure 4d), although always positive, the inter-FC between visual network pairs differed significantly ($F[3.38, 812.6] = 33.67, p < 0.001, \eta^2 = 0.09$). Specifically, inter-FC decreased in strength with increasing frequency (Figure 4d). For example, the inter-FC between Vis-39 and Vis-59 was of 0.83 ($p < 0.0001$) in Slow-5, 0.59 ($p < 0.0001$) in Slow-4, 0.54 ($p < 0.0001$) in Slow-3, but only of 0.06 in Slow-2 ($p = 0.037, n.s.$ after FDR correction).

In summary, we found that the mean inter-FC of CO_n with visual networks was strongest in Slow-4 (negative) and Slow-3 (insula-subcomponent; positive); the mean inter-FC of RFP_n with visual networks was negative and strongest in Slow-5 and Slow-4; the mean inter-FC between CO_n and RFP_n was positive and strongest in Slow-4 and Slow-3 (ACC-subcomponent); and the mean inter-FC between visual networks was positive and strongest in Slow-5. Next, we investigated whether there is an association of VPS C with the inter-FC between these networks and, further, whether this association is frequency specific.

3.3 | Association of VPS parameter *C* with the inter-FC between CON, RFPn, and visual networks

Values for VPS parameter *C* ranged from 10.34 to 47.01 letters per second (mean = 22.90 ± 7.70). We conducted five linear regressions (one for each visual network: Vis-39, Vis-46, Vis-59, Vis-64, and Vis-67) to test the associations between VPS parameter *C* values and the inter-FC of CON and RFPn with visual networks across frequency bins and Global, controlling for age and head motion.

Figure 5 depicts the predictors' beta coefficients (and their corresponding 95% confidence intervals) of inter-FC of CON (a) and RFPn (b) with each visual network across frequency bins (depicted in different colors and geometrical shapes). Significant associations with parameter *C* were found only for the inter-FC of RFPn with two of the five visual networks (Vis-59 and Vis-64) (confidence intervals not including zero; Figure 5b). Specifically, more *negative* inter-FCs of RFPn with Vis-59 (Slow-5: $\beta = -0.56$, SE = 0.22, $p = 0.014$) and Vis-64 (Slow-5: $\beta = -0.56$, SE = 0.22, $p = 0.015$; Slow-2: $\beta = -0.35$, SE = 0.16, $p = 0.034$) were significantly associated with higher VPS parameter *C*. No further significant associations were observed (all p values > 0.060).

To determine possible frequency specificity for the frequency bins that proved significant (i.e., inter-FC of RFPn and Vis-59 in Slow-5 and inter-FC of RFPn and Vis-64 in Slow-5 and Slow-2), we calculated *post-hoc* linear contrasts of the beta coefficients (i.e., Slow-5 > Slow-4; Slow-5 > Slow-3;

Slow-5 > Slow-2; Slow-2 > Slow-4; and Slow-2 > Slow-3). In the regression model of inter-FC between Vis-59 and RFPn (green diamond in Figure 5b), contrasts indicated that the association was significantly different between Slow-5 and Slow-4 ($z = -2.77$, $p = 0.016$), marginally different between Slow-5 and Slow-3 ($z = -2.24$, $p = 0.065$), and not different between Slow-5 and Slow-2 ($p = 0.685$). Similarly, in the model of inter-FC of RFPn with Vis-64 (ocher upward triangle in Figure 5b), the association was significantly different between Slow-5 and Slow-4 ($z = -3.43$, $p = 0.002$) and Slow-2 and Slow-4 ($z = -2.53$, $p = 0.022$), but not between Slow-5 and Slow-3 ($p = 0.102$), Slow-5 and Slow-2 ($p = 0.751$), or Slow-2 and Slow-3 ($p = 0.249$). Thus, the association with VPS parameter *C* observed in Slow-5 for the inter-FC between RFPn and Vis-59 and Vis-64 appears to be also present (although less marked) in Slow-3 and Slow-2, arguing that it is not frequency-specific.

Surprisingly, the inter-FC of CON and visual networks was not significantly associated with VPS parameter *C* in any of the frequency bins and in any of the models (all p values > 0.129; Figure 5a). We also found no significant results for the inter-FC of RFPn or CON with visual networks in Global in any of the models (all p values > 0.158). None of the control variables showed significant associations with VPS parameter *C* in any of the models (age: all p values > 0.255; head motion: all p values > 0.400).

For completeness, we additionally examined the potential link between VPS parameter *C* and the inter-FC between CON and RFPn. We observed a significant association between the

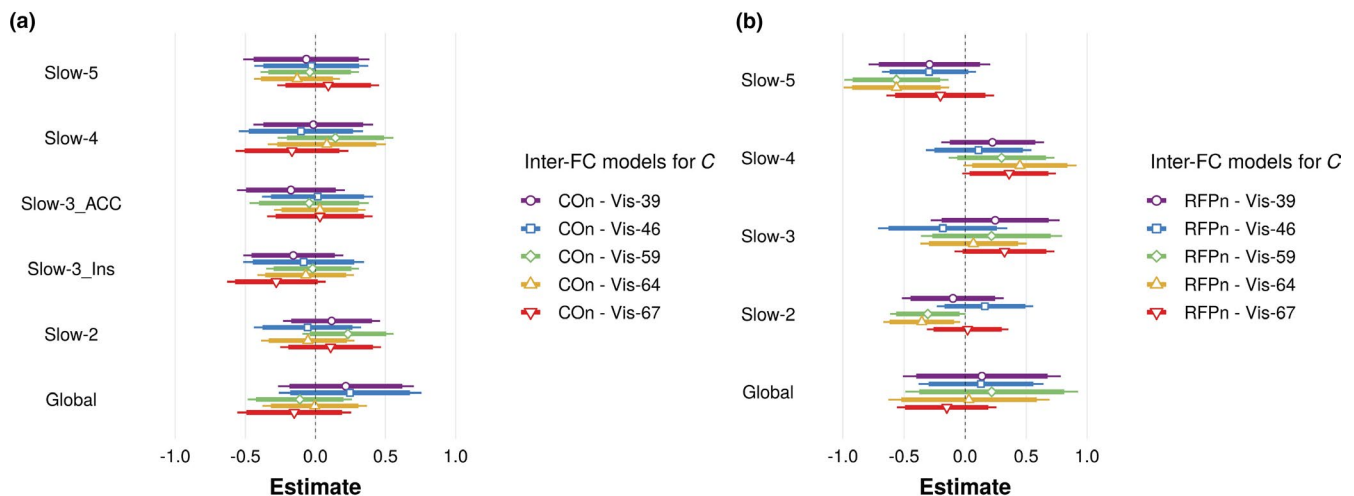


FIGURE 5 Estimates of linear regressions of visual processing speed (VPS) parameter *C* on inter-functional connectivity (inter-FC) of cingulo-opercular network (CON) and right frontoparietal network (RFPn) with visual networks. The standardized coefficients (and their respective 95% confidence intervals) of five multiple regression models of VPS *C* on the inter-FC of CON (a) and RFPn (b) with each visual network (Vis-), are depicted in five different colors and geometrical shapes. All models included as predictors the inter-FC of both CON and RFPn with one of the five visual networks, respectively (hence five regression models), across frequency bins and global, age, and head motion. For clarity, inter-FC predictors are clustered on the y-axis and presented separately for CON (a) and RFPn (b). Estimates of age and head motion, as well as of the intercept, were omitted from the figure for simplicity. Significant estimates are those whose confidence interval does not cross the middle vertical (black dashed) line. Conventions for the regression models: Vis-39: purple, circle; Vis-46: blue, square; Vis-59: green, diamond; Vis-64: ocher, upward triangle; Vis-67: red, downward triangle

inter-FC of CON's ACC-subcomponent and RFPn in Slow-3 only ($\beta = -0.34$, $SE = 0.16$, $p = 0.043$; p values of all other frequency bins and global > 0.269).

In summary, we found higher VPS parameter C to be significantly associated with a more negative inter-FC between RFPn and visual networks in Slow-5 (Vis-59 and Vis-64) and Slow-2 (Vis-64) only. However, contrary to our expectations, we did not find a significant association between VPS parameter C and the inter-FC of CON with visual networks for any frequency bin or global.

4 | DISCUSSION

In this study, we used TVA modeling and a frequency-based approach to systematically investigate whether the between-network functional connectivity (inter-FC) of the cingulo-opercular network (CON) and the right frontoparietal network (RFPn) with visual networks is associated with VPS, building on previous theoretical proposals and exploratory work. We found that inter-FC of RFPn, but not that of CON, with visual networks was linked with VPS, and that this link was also observed beyond the typically analyzed frequency range. Filtering rs-fMRI data into four frequency bins (Slow-5:0.01–0.027 Hz, Slow-4:0.027–0.073 Hz, Slow-3:0.073–0.198 Hz, and Slow-2:0.198–0.4 Hz) revealed a functional subdivision for CON in Slow-3, with the strongest inter-FC with visual networks for CON's insula-subcomponent and the strongest inter-FC with RFPn for CON's ACC-subcomponent. Further, our approach revealed the strongest inter-FC between RFPn and visual networks in the slowest bins (Slow-5 and Slow-4). Our results are indicative of a frequency-specific inter-FC between higher-order and primary resting-state networks relevant for VPS and provide the first empirical evidence for a link between a latent VPS parameter and the intrinsic inter-FC between right frontoparietal (but not frontoinsular) and occipital regions.

4.1 | Inter-FC between RFPn and visual networks links with VPS

We found that the inter-FC between RFPn and visual networks, but not between CON and visual networks, was associated with the VPS parameter (Figure 5). The NTVA (Bundesen et al., 2005) proposes that the computations that determine VPS (i.e., selection of visual features) are generated in frontal, parietal, and/or limbic areas and projected to occipital areas. Previous research based on within-network functional connectivity linked CON and RFPn with VPS (Ruiz-Rizzo et al., 2018). The current study goes beyond by providing the crucial yet missing piece of evidence on whether and how those computations pass onto visual cortices. In addition, our

finer grained approach (in both the temporal and the spatial domain) revealed an association of VPS and inter-FC not only in the typically analyzed frequency range (Slow-5) but, notably, also in frequencies beyond this range (Slow-2 and, less strongly, Slow-3), and for two visual networks (Vis-59 and Vis-64) that include, respectively, dorsal (adjoining parietal cortex) and primary visual areas (Allen et al., 2011). This finding is in accordance with well-established evidence that attentional control signals from (fronto)parietal regions of RFPn modulate sensory processing in visual cortices (Gilbert & Li, 2013; Green & McDonald, 2008; Riedl et al., 2016; Scolari et al., 2015), with evidence of preferential functional connectivity of RFPn regions to primary occipital regions supporting central vision (Griffis et al., 2017), and with evidence that more right-hemispheric lateralization of the inferior fronto-occipital fasciculus associates with higher VPS (Chechlacz et al., 2015). In the present study, inter-FC was measured at rest and the VPS parameter C was obtained independently (i.e., from modeling accuracy in a whole-report task performed on a different day). Accordingly, this association would imply that the *intrinsic* inter-FC with RFPn reflects the individual potential of the visual system to process information in an efficient manner, as the parameter C represents a latent-level measure of VPS (e.g., Finke et al., 2005). Future studies might determine whether there is a functional subdivision within the RFPn whose connectivity with visual areas more accurately represent this efficient processing (akin to the separate pathways that support the control of spatial attention; Szczepanski et al., 2013).

Higher VPS parameter C was associated with *lower* (negative) inter-FC between RFPn and visual networks (Figure 5b; Slow-5 and Slow-2, green and ochre bars). Theoretically, VPS is determined by categorizations, that is, selection of or bias toward visual features (“object x has feature i ”; Bundesen, 1990). In neural terms, such selection increases the firing rate of the cortical neurons coding for a particular feature and, correspondingly, decreases the firing rate of neurons coding for other features (Bundesen et al., 2005). Functional connectivity has been proposed to reflect fluctuations in cortical excitability (Raichle, 2011). Moreover, spontaneous, infra-slow neuronal fluctuations have been shown to underlie functional connectivity (Matsui et al., 2016). Thus, the negative inter-FC between RFPn and visual networks (observed in Slow-5 and Slow-2) suggests a neural implementation of the category selection mechanism—a visual categorization would increase the activity of, specifically, the visual areas coding for a particular feature, but not of *all* visual areas (coding other features and where activity would decrease), thereby translating into a net decrease.

The inter-FC between CON and visual networks was not associated with VPS parameter C , contrary to what we expected and unlike RFPn. One possibility for this null finding may be that CON's functional role in sustained

cognitive control (see below) is not limited solely to visual processing and requires more interaction with higher order networks (e.g., to control switching between default mode and central executive networks; Sridharan et al., 2008) than with unimodal networks. This possibility is further supported by our finding of an association of the inter-FC between CON and RFPn with VPS, also shown previously in an exploratory analysis that aimed to shed light on the functional connectivity *within* CON (Ruiz-Rizzo et al., 2018). CON and RFPn are two functionally well coupled but distinct networks associated with cognitive control (e.g., Crittenden et al., 2016; Dosenbach et al., 2007). Whereas CON has been suggested to be involved in cognitive control across longer periods of time, RFPn appears to adjust control more rapidly and dynamically (Dosenbach et al., 2008; Sadaghiani et al., 2012). The functional connectivity *within* CON and its *inter*-FC with RFPn have previously been shown relevant for the VPS parameter *C* in an independent sample of young adults (e.g., Ruiz-Rizzo et al., 2018). In light of this previous evidence, the new findings allow us to propose a possible functional hierarchy among intrinsic networks relevant for the latent parameter VPS. In detail, while sustaining cognitive control in a visual task, CON might require RFPn to respond (in a phasic manner) to incoming stimuli, and RFPn would thereby enhance stimulus processing in visual (primary and dorsal occipital) regions. Assessing effective (i.e., directional) FC could provide further empirical support to this proposal.

4.2 | Inter-FC between VPS relevant networks is frequency-specific

Previous studies showed that resting-state networks can be observed at frequencies beyond the traditionally examined frequency range (0.01–0.1 Hz) and that filtering data to this range discards potential differences in functional connectivity (Gohel & Biswal, 2015; Kalcher et al., 2014; Wang et al., 2018; Zuo et al., 2010). Accordingly, we followed a frequency-based approach, which yielded two main insights. First, there was a meaningful subdivision of CON in Slow-3 into its two core regions (e.g., Seeley et al., 2007), the insula and the ACC. This subdivision showed a particular inter-FC pattern, with significant inter-FC of the *insula*-subcomponent with visual networks and significant inter-FC of the *ACC*-subcomponent with RFPn. Of note, this subdivision only occurred in Slow-3 (also see Salvador et al., 2008), which includes frequencies typically filtered out (e.g., >0.1), and is in agreement with task-fMRI evidence of a functional dissociation between the insula (alerting) and the ACC (set switching) (Han et al., 2019) and previous rs-fMRI evidence of the intrinsic connectivity of the (posterior dorsal) insula with visual brain areas (Cauda et al., 2011).

Second, the average inter-FC of CON and RFPn with all visual networks appears stronger in some frequencies (Figure 4), though it is present across all frequency bins (Figure 3) (see also, Gohel & Biswal, 2015). For CON, the strongest average inter-FC with visual networks was found in Slow-4 (upper typical range) and Slow-3 (faster than the typically analyzed rs-fMRI BOLD signal frequency range), whereas for RFPn, the strongest average inter-FC with visual networks was found in Slow-5 and Slow-4 (the typically analyzed frequency range), aligning well with previous evidence on brain-regional differences in frequency power (e.g., Baria et al., 2011). The strongest inter-FC between visual network pairs was found in Slow-5, in accordance with previous documentations that the fMRI-BOLD signal in occipital networks mostly concentrates in infra-slow frequencies (i.e., 0.01–0.06 Hz; Wu et al., 2008; Baria et al., 2011) and correlates positively with lower frequency electroencephalographic amplitude (i.e., delta and theta rhythms; ~1.0–8.2 Hz; Jann et al., 2010). From a methods perspective, the previous documentations, along with the found association between the inter-FC of RFPn with visual networks in Slow-2 and VPS parameter *C*, provide supportive evidence that a frequency-binned approach can yield additional, valuable insights into the rs-fMRI BOLD signal. Accordingly, combining the frequencies altogether without binning (i.e., “Global”) cancels out any specificity in inter-FC or the association of inter-FC with VPS.

In interpreting our results, some limitations should be considered. First, the two CON subcomponents were identified only in Slow-3. Future studies should determine whether this separation is specific to Slow-3 or CON. Further, the results on the strongest inter-FC in specific frequency bins do not directly imply “communication” preferences between the neuronal populations of those networks. Rather, inter-FC was observed across the entire spectrum measured with BOLD-fMRI, which is in line with electrophysiological evidence showing that the oscillations that characterize functional networks span multiple frequency bands (Mantini et al., 2007). Finally, task-based fMRI studies investigating VPS variability *within* an individual could help elucidate the meaning and relevance of the observed negative association between inter-FC (of RFPn and visual networks) and VPS. Despite its limitations, our study underscores the usefulness of a frequency-based approach for better understanding the spontaneous fMRI-BOLD activity and how it links to behavior (Kalcher et al., 2014; Sasai et al., 2014; Wu et al., 2008).

5 | CONCLUSION

Our study provides first empirical evidence that the intrinsic inter-FC between RFPn and visual networks links to VPS. Albeit expected, we did not find such a link for

CO. Our systematic frequency-based approach revealed that the inter-FC between functional networks relevant for VPS and their link to VPS are also observed in frequencies above 0.1 Hz.

ETHICS APPROVAL STATEMENT

The study was approved by the ethics committee of the Faculty of Psychology and Educational Sciences of LMU Munich, and all participants provided written informed consent.

ACKNOWLEDGEMENTS

We thank Dr Mario E. Archila-Meléndez for helpful feedback on an earlier version of this paper and Dr Julia Neitzel for participant recruitment.

CONFLICT OF INTEREST

The authors declare no competing financial interests.

AUTHOR CONTRIBUTIONS

S. K.: formal analysis; validation; visualization; writing—original draft. C. S.: conceptualization; funding acquisition; supervision; writing—review and editing. S. S.: formal analysis; writing—review and editing. O. K.: formal analysis; writing—review and editing. H. M.: funding acquisition; supervision; writing—review and editing. N. N.: investigation; resources. A. M.: investigation. K. F.: conceptualization; funding acquisition; supervision; writing—review and editing. A. R.: conceptualization; investigation; data curation; formal analysis; validation; visualization; writing—original draft.

PEER REVIEW

The peer review history for this article is available at <https://publons.com/publon/10.1111/ejn.15206>.

DATA AVAILABILITY STATEMENT

The data that support the findings of this study are openly available in OSF (<https://doi.org/10.17605/OSF.IO/NHQG3>). The behavioral data are available on request from the corresponding author.

ORCID

Adriana L. Ruiz-Rizzo  <https://orcid.org/0000-0003-1467-0745>

REFERENCES

Allen, E. A., Erhardt, E. B., Damaraju, E., Gruner, W., Segall, J. M., Silva, R. F., Havlicek, M., Rachakonda, S., Fries, J., Kalyanam, R., Michael, A. M., Caprihan, A., Turner, J. A., Eichele, T., Adelsheim, S., Bryan, A. D., Bustillo, J., Clark, V. P., Feldstein Ewing, S. W., ... Calhoun, V. D. (2011). A baseline for the multivariate comparison of resting-state networks. *Frontiers in Systems Neuroscience*, 5, <https://doi.org/10.3389/fnsys.2011.00002>

Ashburner, J. (2007). A fast diffeomorphic image registration algorithm. *NeuroImage*, 38(1), 95–113. <https://doi.org/10.1016/j.neuroimage.2007.07.007>

Baria, A. T., Baliki, M. N., Parrish, T., & Apkarian, A. V. (2011). Anatomical and functional assemblies of brain BOLD oscillations. *Journal of Neuroscience*, 31(21), 7910–7919. <https://doi.org/10.1523/JNEUROSCI.1296-11.2011>

Beall, E. B., & Lowe, M. J. (2007). Isolating physiologic noise sources with independently determined spatial measures. *NeuroImage*, 37(4), 1286–1300. <https://doi.org/10.1016/j.neuroimage.2007.07.004>

Beckmann, C. F., Mackay, C. E., Filippini, N., & Smith, S. M. (2009). Group comparison of resting-state FMRI data using multi-subject ICA and dual regression. *NeuroImage*, 47(Suppl 1), S148. [https://doi.org/10.1016/S1053-8119\(09\)71511-3](https://doi.org/10.1016/S1053-8119(09)71511-3)

Benjamini, Y., & Hochberg, Y. (1995). Controlling the false discovery rate: A practical and powerful approach to multiple testing. *Journal of the Royal Statistical Society: Series B (Methodological)*, 57(1), 289–300.

Bundesen, C. (1990). A theory of visual attention. *Psychological Review*, 97(4), 523–547. <https://doi.org/10.1037/0033-295X.97.4.523>

Bundesen, C., Habekost, T., & Kyllingsbæk, S. (2005). A neural theory of visual attention: Bridging cognition and neurophysiology. *Psychological Review*, 112(2), 291–328. <https://doi.org/10.1037/0033-295X.112.2.291>

Cauda, F., D'Agata, F., Sacco, K., Duca, S., Geminiani, G., & Vercelli, A. (2011). Functional connectivity of the insula in the resting brain. *NeuroImage*, 55(1), 8–23. <https://doi.org/10.1016/j.neuroimage.2010.11.049>

Chechlacz, M., Gillebert, C. R., Vangkilde, S. A., Petersen, A., & Humphreys, G. W. (2015). Structural variability within frontoparietal networks and individual differences in attentional functions: An approach using the theory of visual attention. *Journal of Neuroscience*, 35(30), 10647–10658. <https://doi.org/10.1523/JNEUROSCI.0210-15.2015>

Cordes, D., Haughton, V. M., Arfanakis, K., Carew, J. D., Turski, P. A., Moritz, C. H., Quigley, M. A., & Meyerand, M. E. (2001). Frequencies contributing to functional connectivity in the cerebral cortex in “Resting-state” data. *American Journal of Neuroradiology*, 22(7), 1326–1333.

Crittenden, B. M., Mitchell, D. J., & Duncan, J. (2016). Task encoding across the multiple demand cortex is consistent with a frontoparietal and cingulo-opercular dual networks distinction. *The Journal of Neuroscience*, 36(23), 6147–6155. <https://doi.org/10.1523/JNEUROSCI.4590-15.2016>

Deutsche Bearbeitung von Beck, A.T., von Beck, A. T., Steer, R. A., & Brown, G. K. (1996). *Beck depression inventory-II (BDI-II)*. San Antonio, TX: Psychological Corporation.

Dosenbach, N. U. F., Fair, D. A., Cohen, A. L., Schlaggar, B. L., & Petersen, S. E. (2008). A dual-networks architecture of top-down control. *Trends in Cognitive Sciences*, 12(3), 99–105. <https://doi.org/10.1016/j.tics.2008.01.001>

Dosenbach, N. U. F., Fair, D. A., Miezin, F. M., Cohen, A. L., Wenger, K. K., Dosenbach, R. A. T., Fox, M. D., Snyder, A. Z., Vincent, J. L., Raichle, M. E., Schlaggar, B. L., & Petersen, S. E. (2007). Distinct brain networks for adaptive and stable task control in humans. *Proceedings of the National Academy of Sciences*, 104(26), 11073–11078. <https://doi.org/10.1073/pnas.0704320104>

Dyrholm, M., Kyllingsbæk, S., Espeseth, T., & Bundesen, C. (2011). Generalizing parametric models by introducing trial-by-trial parameter

- variability: The case of TVA. *Journal of Mathematical Psychology*, 55(6), 416–429. <https://doi.org/10.1016/j.jmp.2011.08.005>
- Finke, K., Bublak, P., Krummenacher, J., Kyllingsbæk, S., Müller, H. J., & Schneider, W. X. (2005). Usability of a theory of visual attention (TVA) for parameter-based measurement of attention I: Evidence from normal subjects. *Journal of the International Neuropsychological Society*, 11(07), <https://doi.org/10.1017/S1355617705050976>
- Gilbert, C. D., & Li, W. (2013). Top-down influences on visual processing. *Nature Reviews Neuroscience*, 14(5), 350–363. <https://doi.org/10.1038/nrn3476>
- Gohel, S. R., & Biswal, B. B. (2015). Functional integration between brain regions at rest occurs in multiple-frequency bands. *Brain Connectivity*, 5(1), 23–34. <https://doi.org/10.1089/brain.2013.0210>
- Green, J. J., & McDonald, J. J. (2008). Electrical neuroimaging reveals timing of attentional control activity in human brain. *PLoS Biology*, 6(4), e81. <https://doi.org/10.1371/journal.pbio.0060081>
- Griffis, J. C., Elkhatali, A. S., Burge, W. K., Chen, R. H., Bowman, A. D., Szaflarski, J. P., & Visscher, K. M. (2017). Retinotopic patterns of functional connectivity between V1 and large-scale brain networks during resting fixation. *NeuroImage*, 146, 1071–1083. <https://doi.org/10.1016/j.neuroimage.2016.08.035>
- Han, S. W., Eaton, H. P., & Marois, R. (2019). Functional Fractionation of the Cingulo-opercular Network: Alerting Insula and Updating Cingulate. *Cerebral Cortex*, 29(6), 2624–2638. <https://doi.org/10.1093/cercor/bhy130>
- Haupt, M., Ruiz-Rizzo, A. L., Sorg, C., & Finke, K. (2020). Right-lateralized fronto-parietal network and phasic alertness in healthy aging. *Scientific Reports*, 10(1), 4823. <https://doi.org/10.1038/s41598-020-61844-z>
- Hautzinger, M., Keller, F., & Kühner, C. (2009). *Beck depressions-inventar (BDI-II)*. Revision. Frankfurt am Main: Pearson.
- Jann, K., Koenig, T., Dierks, T., Boesch, C., & Federspiel, A. (2010). Association of individual resting state EEG alpha frequency and cerebral blood flow. *NeuroImage*, 51(1), 365–372. <https://doi.org/10.1016/j.neuroimage.2010.02.024>
- Jenkinson, M., Beckmann, C. F., Behrens, T. E. J., Woolrich, M. W., & Smith, S. M. (2012). *FSL*. *Neuroimage*, 62(2), 782–790. <https://doi.org/10.1016/j.neuroimage.2011.09.015>
- Kalcher, K., Boubela, R. N., Huf, W., Bartova, L., Kronnerwetter, C., Derntl, B., Pezawas, L., Filzmoser, P., Nasel, C., & Moser, E. (2014). The Spectral Diversity of Resting-State Fluctuations in the Human Brain. *PLoS One*, 9(4), e93375. <https://doi.org/10.1371/journal.pone.0093375>
- Kyllingsbæk, S. (2006). Modeling visual attention. *Behavior Research Methods*, 38(1), 123–133. <https://doi.org/10.3758/BF03192757>
- Lehrl, S., Merz, J., Burkhard, G., & Fischer, S. (1999). *Mehrfachwahl-Wortschatz-Intelligenztest*. MWT-B, 4th ed. Spitta.
- Mantini, D., Perucci, M. G., Gratta, C. D., Romani, G. L., & Corbetta, M. (2007). Electrophysiological signatures of resting state networks in the human brain. *Proceedings of the National Academy of Sciences*, 104(32), 13170–13175. <https://doi.org/10.1073/pnas.0700668104>
- Matsui, T., Murakami, T., & Ohki, K. (2016). Transient neuronal co-activations embedded in globally propagating waves underlie resting-state functional connectivity. *Proceedings of the National Academy of Sciences*, 113(23), 6556–6561. <https://doi.org/10.1073/pnas.1521299113>
- McAvinue, L. P., Habekost, T., Johnson, K. A., Kyllingsbæk, S., Vangkilde, S., Bundesen, C., & Robertson, I. H. (2012). Sustained attention, attentional selectivity, and attentional capacity across the lifespan. *Attention, Perception, & Psychophysics*, 74(8), 1570–1582. <https://doi.org/10.3758/s13414-012-0352-6>
- Mckeown, M. J., Makeig, S., Brown, G. G., Jung, T.-P., Kindermann, S. S., Bell, A. J., & Sejnowski, T. J. (1998). Analysis of fMRI data by blind separation into independent spatial components. *Human Brain Mapping*, 6(3), 160–188. [https://doi.org/10.1002/\(SICI\)1097-0193\(1998\)6:3<160::AID-HBM5>3.0.CO;2-1](https://doi.org/10.1002/(SICI)1097-0193(1998)6:3<160::AID-HBM5>3.0.CO;2-1)
- Penny, W. D., Friston, K. J., Ashburner, J. T., Kiebel, S. J., & Nichols, T. E. (2011). *Statistical Parametric Mapping: The Analysis of Functional Brain Images*. Elsevier.
- Penttonen, M., & Buzsáki, G. (2003). Natural logarithmic relationship between brain oscillators. *Thalamus & Related Systems*, 2(2), 145–152. [https://doi.org/10.1016/S1472-9288\(03\)00007-4](https://doi.org/10.1016/S1472-9288(03)00007-4)
- Power, J. D., Barnes, K. A., Snyder, A. Z., Schlaggar, B. L., & Petersen, S. E. (2012). Spurious but systematic correlations in functional connectivity MRI networks arise from subject motion. *NeuroImage*, 59(3), 2142–2154. <https://doi.org/10.1016/j.neuroimage.2011.10.018>
- Preibisch, C., Castrillón G., J. G., Bührer, M., & Riedl, V. (2015). Evaluation of multiband EPI acquisitions for resting state fMRI. *PLoS One*, 10(9), e0136961. <https://doi.org/10.1371/journal.pone.0136961>
- R Core Team (2020). *R: The R Project for Statistical Computing*. <https://www.r-project.org/>
- Raichle, M. E. (2011). *The Restless Brain*. *Brain Connectivity*, 1(1), 3–12. <https://doi.org/10.1089/brain.2011.0019>
- Reitan, R. M. (1958). *Validity of the Trail Making Test as an Indicator of Organic Brain Damage.*, 84, 6.
- Riedl, V., Utz, L., Castrillón, G., Grimmer, T., Rauschecker, J. P., Ploner, M., Friston, K. J., Drzezga, A., & Sorg, C. (2016). Metabolic connectivity mapping reveals effective connectivity in the resting human brain. *Proceedings of the National Academy of Sciences*, 113(2), 428–433. <https://doi.org/10.1073/pnas.1513752113>
- Ries, A., Chang, C., Glim, S., Meng, C., Sorg, C., & Wohlschläger, A. (2018). Grading of frequency spectral centroid across resting-state networks. *Frontiers in Human Neuroscience*, 12, <https://doi.org/10.3389/fnhum.2018.00436>
- Ruiz-Rizzo, A. L., & Küchenhoff, S. (2020). *Inter-FC*. <https://osf.io/nhqg3/>
- Ruiz-Rizzo, A. L., Neitzel, J., Müller, H. J., Sorg, C., & Finke, K. (2018). Distinctive correspondence between separable visual attention functions and intrinsic brain networks. *Frontiers in Human Neuroscience*, 12, <https://doi.org/10.3389/fnhum.2018.00089>
- Ruiz-Rizzo, A. L., Sorg, C., Napiórkowski, N., Neitzel, J., Menegaux, A., Müller, H. J., Vangkilde, S., & Finke, K. (2019). Decreased cingulo-opercular network functional connectivity mediates the impact of aging on visual processing speed. *Neurobiology of Aging*, 73, 50–60. <https://doi.org/10.1016/j.neurobiolaging.2018.09.014>
- Sadaghiani, S., Scheeringa, R., Lehongre, K., Morillon, B., Giraud, A.-L., D'Esposito, M., & Kleinschmidt, A. (2012). Alpha-band phase synchrony is related to activity in the fronto-parietal adaptive control network. *Journal of Neuroscience*, 32(41), 14305–14310. <https://doi.org/10.1523/JNEUROSCI.1358-12.2012>
- Salvador, R., Martínez, A., Pomarol-Clotet, E., Gomar, J., Vila, F., Sarró, S., Capdevila, A., & Bullmore, E. (2008). A simple view of the brain through a frequency-specific functional connectivity measure. *NeuroImage*, 39(1), 279–289. <https://doi.org/10.1016/j.neuroimage.2007.08.018>

- Sasai, S., Homae, F., Watanabe, H., Sasaki, A. T., Tanabe, H. C., Sadato, N., & Taga, G. (2014). Frequency-specific network topologies in the resting human brain. *Frontiers in Human Neuroscience*, *8*, <https://doi.org/10.3389/fnhum.2014.01022>
- Scolari, M., Seidl-Rathkopf, K. N., & Kastner, S. (2015). Functions of the human frontoparietal attention network: Evidence from neuroimaging. *Current Opinion in Behavioral Sciences*, *1*, 32–39. <https://doi.org/10.1016/j.cobeha.2014.08.003>
- Seeley, W. W., Menon, V., Schatzberg, A. F., Keller, J., Glover, G. H., Kenna, H., Reiss, A. L., & Greicius, M. D. (2007). Dissociable intrinsic connectivity networks for salience processing and executive control. *Journal of Neuroscience*, *27*(9), 2349–2356. <https://doi.org/10.1523/JNEUROSCI.5587-06.2007>
- Sestieri, C., Corbetta, M., Spadone, S., Romani, G. L., & Shulman, G. L. (2013). Domain-general signals in the Cingulo-opercular network for visuospatial attention and episodic memory. *Journal of Cognitive Neuroscience*, *26*(3), 551–568. https://doi.org/10.1162/jocn_a_00504
- Smith, S. M., Jenkinson, M., Woolrich, M. W., Beckmann, C. F., Behrens, T. E. J., Johansen-Berg, H., Bannister, P. R., De Luca, M., Drobnjak, I., Flitney, D. E., Niazy, R. K., Saunders, J., Vickers, J., Zhang, Y., De Stefano, N., Brady, J. M., & Matthews, P. M. (2004). Advances in functional and structural MR image analysis and implementation as FSL. *NeuroImage*, *23*, S208–S219. <https://doi.org/10.1016/j.neuroimage.2004.07.051>
- Sperling, G. (1960). The information available in brief visual presentations. *Psychological Monographs: General and Applied*, *74*(11), 1–29. <https://doi.org/10.1037/h0093759>
- Sridharan, D., Levitin, D. J., & Menon, V. (2008). A critical role for the right fronto-insular cortex in switching between central-executive and default-mode networks. *Proceedings of the National Academy of Sciences*, *105*(34), 12569–12574. <https://doi.org/10.1073/pnas.0800005105>
- Szczepanski, S. M., Pinsk, M. A., Douglas, M. M., Kastner, S., & Saalman, Y. B. (2013). Functional and structural architecture of the human dorsal frontoparietal attention network. *Proceedings of the National Academy of Sciences*, *110*(39), 15806–15811. <https://doi.org/10.1073/pnas.1313903110>
- Thiebaut de Schotten, M., Dell'Acqua, F., Forkel, S., Simmons, A., Vergani, F., Murphy, D. G. M., & Catani, M. (2011). A lateralized brain network for visuo-spatial attention. *Nature Precedings*, *1–1*, <https://doi.org/10.1038/npre.2011.5549.1>
- Tombaugh, T. N. (2004). Trail making test A and B: Normative data stratified by age and education. *Archives of Clinical Neuropsychology*, *19*(2), 203–214. [https://doi.org/10.1016/S0887-6177\(03\)00039-8](https://doi.org/10.1016/S0887-6177(03)00039-8)
- Uddin, L. Q., Yeo, B. T. T., & Spreng, R. N. (2019). Towards a universal taxonomy of macro-scale functional human brain networks. *Brain Topography*, *32*(6), 926–942. <https://doi.org/10.1007/s10548-019-00744-6>
- Wang, Y., Zhu, L., Zou, Q., Cui, Q., Liao, W., Duan, X., Biswal, B., & Chen, H. (2018). Frequency dependent hub role of the dorsal and ventral right anterior insula. *NeuroImage*, *165*, 112–117. <https://doi.org/10.1016/j.neuroimage.2017.10.004>
- Wu, C. W., Gu, H., Lu, H., Stein, E. A., Chen, J.-H., & Yang, Y. (2008). Frequency specificity of functional connectivity in brain networks. *NeuroImage*, *42*(3), 1047–1055. <https://doi.org/10.1016/j.neuroimage.2008.05.035>
- Yan, C., & Zang, Y. (2010). DPARSF: A MATLAB toolbox for “pipeline” data analysis of resting-state fMRI. *Frontiers in Systems Neuroscience*, *4*, <https://doi.org/10.3389/fnsys.2010.00013>
- Zuo, X.-N., Di Martino, A., Kelly, C., Shehzad, Z. E., Gee, D. G., Klein, D. F., Castellanos, F. X., Biswal, B. B., & Milham, M. P. (2010). The oscillating brain: Complex and reliable. *NeuroImage*, *49*(2), 1432–1445. <https://doi.org/10.1016/j.neuroimage.2009.09.037>

How to cite this article: Küchenhoff S, Sorg C, Schneider S, et al. Visual processing speed is linked to functional connectivity between right frontoparietal and visual networks. *Eur J Neurosci*. 2021;53:3362–3377. <https://doi.org/10.1111/ejn.15206>